Glioma-induced caspase 3 inhibition in microglia promotes a tumor-supportive phenotype

Xianli Shen[1,15], Miguel A. Burguillos[1,11,15], Ahmed M. Osman[2,3], Jeroen Frijhoff[1,12], Alejandro Carrillo-Jiménez[4,5], Sachie Kanatani[6,7], Martin Augsten[1,13], Dalel Saidi[1], Johanna Rodhe[1], Edel Kavanagh[1], Anthony Rongvaux[8,14], Vilma Rraklli[9], Ulrika Nyman[9], Johan Holmberg[9], Arne Östman[1], Richard A. Flavell[8,10], Antonio Barragan[6,7], Jose Luis Venero[4,5], Klas Blomgren[2,3] and Bertrand Joseph[1,16].

[1]Department of Oncology-Pathology, Cancer Centrum Karolinska, Karolinska Institutet, Stockholm, Sweden

[2]Department of Women's and Children's Health, Karolinska Institutet, Karolinska University Hospital, Stockholm, Sweden

[3]Department of Pediatric Oncology, Karolinska University Hospital, Stockholm, Sweden

[4]Departamento de Bioquímica y Biología Molecular, Universidad de Sevilla, Sevilla, Spain

[5]Instituto de Biomedicina de Sevilla, Hospital Universitario Virgen del Rocío/CSIC/Universidad de Sevilla, Sevilla, Spain

[6]Center for Infectious Medicine, Department of Medicine, Karolinska Institutet, Stockholm, Sweden

[7]Department of Molecular Biosciences, the Wenner-Gren Institute, Stockholm University, Stockholm, Sweden

[8]Department of Immunobiology, Yale University School of Medicine, New Haven, CT, USA

[9]Department of Cell and Molecular Biology, Ludwig Institute for Cancer Research, Karolinska Institutet, Stockholm, Sweden

[10]Howard Hughes Medical Institute, Yale University School of Medicine, New Haven, CT, USA

[11]Present address: Centre for Neuroscience and Trauma, Blizard Institute, Queen Mary University of London, London E1 2AT, United Kingdom

[12]Present address: Department of Pharmacology and Personalised Medicine, CARIM, Maastricht, The Netherlands

[13]Present address: Division for vascular Oncology and Metastasis, German Cancer Research Center (DKFZ), Heidelberg, Germany

[14]Present address: Program in Immunology, Fred Hutchinson Cancer Center, Seattle, WA, USA

[15]Co-first author

[16] Correspondence should be addressed to B.J. (Bertrand.Joseph@ki.se)

Abstract

Glioma cells recruit and exploit microglia, resident immune cells of the brain, for their proliferation and invasion capability. The underlying molecular mechanism used by glioma cells to transform microglia into a tumor-supporting phenotype remains elusive. Here we report that glioma-induced microglia conversion is coupled to a reduction of basal microglial caspase 3 activity, increased S-nitrosylation of mitochondria-associated caspase 3 through inhibition of thioredoxin 2 (Trx2) activity, and demonstrate that caspase 3 inhibition regulates microglial tumor-supporting function. Further, we identified nitric oxide synthase 2 (NOS2) activity originating from the glioma cells as a driving stimulus in the control of microglial caspase 3 activity. Repression of glioma NOS2 expression *in vivo* led to reduction in both microglia recruitment and tumor expansion, whereas depletion of the microglial caspase 3 gene promoted tumor growth. This study provides evidence that the inhibition of Trx2-mediated denitrosylation of SNO-procaspase 3 is part of the microglial pro-tumoral activation pathway initiated by glioma cancer cells.

Microglia are necessary for brain development and to maintain normal brain physiology. However, when brain homeostasis is perturbed, microglia react and execute immune functions. In the context of diseases, activation of microglia can contribute to rather contrasting effects; promoting neuronal cell death in the case of neurodegenerative diseases, such as Alzheimer's and Parkinson's diseases, but promoting cell growth and invasion in the case of glioma[1, 2]. In fact, microglia are attracted toward gliomas in large numbers and microglia density in gliomas positively correlates with malignancy, invasiveness and grading of tumors. Tumor cells shut down the inflammatory properties of microglia and modulate them to exert tumor-trophic functions. Microglia release several factors, including extracellular matrix proteases and cytokines, which in turn directly or indirectly influence tumor invasiveness and growth[1, 2]. As further evidence of

their essential role in glioma progression, removal of microglia, both in brain organotypic slices and genetic mouse models, inhibited glioma invasiveness[3, 4]. Moreover, targeting cells in the glioma microenvironment, such as tumor-associated macrophages and microglia, has been proposed as an intervention to combat glioma expansion[5, 6] . Therefore, deciphering the molecular mechanisms that provide the control of microglia activation toward a tumor-supporting phenotype in response to cues from glioma cells is of considerable interest. It was previously shown that a caspase-dependent signaling pathway controlled microglia pro-inflammatory activation and associated neurotoxicity. It was demonstrated that the orderly activation of caspase 8, and thereafter caspase 3 and caspase 7, commonly known to have executioner roles in apoptosis, can promote pro-inflammatory activation of microglia in the absence of cell death[7]. Hence, here we decided to explore whether glioma-induced microglia activation involves caspase-dependent signaling pathways. Here we describe that S-nitrosylation of microglial caspase 3 induced by glioma cells contributes to polarization of microglia into a tumor supportive phenotype necessary for glioma expansion.

Results

Glioma cells decrease basal caspase 3 activity in microglia

Using a segregated coculture transwell set-up (**Supplementary Fig.1a**), DEVDase activity, which reflects caspase 3 like enzymatic activities, was examined in mouse BV2 microglia cells stimulated by soluble factors originating from glioma cells of different origin. Basal DEVDase activity was found to be reduced in the BV2 microglia cells upon segregated coculture with C6 glioma cells (**Fig.1a**); an effect also observed upon joined coculture conditions (**Fig.1b**). Decreased microglial caspase 3 like enzymatic activity upon exposure to glioma-derived soluble factors was further confirmed with additional segregated coculture combinations with the human CHME3 microglia cell line (**Fig.1c**), and mouse or human primary microglia (**Fig.1d**), and a panel of glioma cell lines of

different origin (human U-251MG, U-343MG, U-373MG, U-1241MG cells, U-87MG and murine GL261 cells) (**Fig.1a-d**). In contrast, caspase-8 enzymatic activity as measured by LETDase activity, was found to be mostly unaffected in BV2 microglia cells upon segregated coculture with glioma cells (**Supplementary Fig.1b**), suggesting that the suppression of caspase 3 like activity is independent of caspase-8 activity. Noteworthy, it was previously reported that the pro-inflammatory activation of microglia relies on successive activation of caspase-8 and caspase 3 (Ref. 7), indicating that polarization of microglia cells toward a tumor-supporting phenotype depends on a distinct signaling pathway. Confirming the soluble nature of the stimulus released by the glioma cells, conditioned medium from C6 cells reduced DEVDase activity in both BV2 microglia and primary microglia isolated from murine cortex (**Fig.1e**). The decrease in microglial basal caspase-3-like activity observed upon microglia-glioma segregated coculture correlates with a reduction in the expression of the active p19 subunit of caspase 3 (**Fig.1f**) and a corresponding increase in the expression of its inactive zymogene, procaspase 3 (**Fig.1g**)[8, 9]. To examine the physiological relevance of these findings, we performed *in vivo* experiments and injected GFP-expressing GL261 glioblastoma cells into the brain of young C57/BL6/J mice (**Supplementary Fig.1c**)[10, 11]. Importantly, this syngeneic transplant tumor model in immunocompetent mice has been shown, at the time points used, to exhibit limited infiltration by peripheral monocytes or macrophages[12]. Immunohistochemical analysis of brain tissue surrounding the grown gliomas at 1 and 2 weeks post-transplantation, revealed a massive recruitment of Iba-1 expressing microglia cells and the expression of cleaved caspase 3 in microglia cells was significantly lower in cells localized inside the tumor mass as compared to cells residing at the periphery of the tumor (**Fig.1h-j**). We validated this decrease in the expression of microglial cleaved caspase 3 inside the tumor in another transplant tumor model where human U87-MG glioblastoma cells were injected into NOD.SCID mice brains and microglia response were analyzed. Immunohistochemical analysis of brain tissue, including the formed glioma tumors 1 week post-transplantation, revealed low or absent expression of cleaved caspase 3 in microglia cells localized inside the tumor mass

(**Supplementary Fig.2a,b**). In conclusion, the data obtained from human and murine originating microglia and glioma cells, and the *in vivo* experiments in two different transplant tumor models, support the idea of glioma inhibiting microglial basal caspase 3 activity.

Caspase 3 knockdown promotes a tumor-supportive phenotype

We hypothesized that the observed down-regulation of microglial caspase 3 activity, in response to a glioma stimulus, contributes to the polarization of the microglia cells toward their tumor-promoting functions. We therefore decided to assess the role of caspase 3 in the activation of BV2 microglia by knocking down endogenous procaspase 3 using a pool of siRNAs (**Fig.2a**), mimicking the effect of glioma cells on basal microglial DEVDase activity (**Fig.2b**). BV2 monocultures and those in segregated cocultures with C6 glioma cells were used for comparisons. Microglia activation was assessed using a mouse wound healing RT² profiler PCR array, which encompasses 84 key genes central to the wound healing response. Many of these signaling pathways and associated functions are shared with the pro-tumorigenic phenotype of myeloid cells, as they can promote cell proliferation, tissue remodeling, angiogenesis and the development of an immunosuppressive environment[13]. The gene expression array revealed that silencing caspase 3 *per se* in microglia was able to trigger a tumor-supportive like phenotype and even to synergize with the stimulating effects of glioma cells (**Fig.2c**). The most significant hit, interleukin-6 (IL6) is relevant in a clinical context, since elevated IL6 expression is associated with poor glioma patient survival[14]. IL6 signaling appears to contribute to glioma malignancy through the promotion of glioma stem cell growth and survival[14]. In addition, IL6 participates in the maintenance of the microglial tumor-supportive functions[15]. Induction of *Il6* mRNA expression and three additional markers associated with the microglial tumor-supportive phenotype (not included in the above array), the chemokine *Ccl22*, the chitinase-like molecule *Chil3* (also known as *Ym1*), and the matrix metalloproteinase *Mmp14* (Ref. 4) were further confirmed by qPCR analysis upon coculture with C6 or GL261 glioma cells (**Fig. 2d** and **Supplementary Fig.3**).

Microglial *Nos2* expression, whose induction is strongly associated with the pro-inflammatory phenotype of these cells, was shown to be significantly decreased upon caspase 3 knockdown and even abrogated upon coculture with C6 glioma (**Fig.2d** and **Supplementary Fig.3**). Using transwell cell migration and invasion assays, we examined whether the inhibition of caspase 3 by selective knockdown in microglia was associated with increased glioma motility and invasiveness. As previously shown, microglia caused an increase in glioma mobility and invasiveness[1, 2]. We observed that reducing microglial caspase 3 expression increases migratory and invasive functions in glioma cells (**Fig.2e**). Microglia cells are recruited in an activated state before being converted into tumor-supporting cells by the glioma cells[16, 17]. Therefore, in order to assess the strength of the glioma-mediated microglial caspase 3 repression and its impact on the polarization of the microglia toward a pro-tumor phenotype, BV2 cells were pre-treated with lipopolysaccharide (LPS) for 24 hours before being challenged in a glioma coculture set up for an additional 6 hours (**Fig.3a-d**). It was previously reported that LPS treatment induces DEVDase activity in microglia and that this activity is linked to microglial pro-inflammatory activation[7]. Glioma cells diminished LPS-induced active caspase 3 subunit expression and associated enzymatic activity (**Fig.3a,c**). In contrast, we found that LPS-induced microglial caspase-8 activity (LETDase) was unaffected by the presence of glioma cells (**Fig.3b**). In accordance with this, glioma cells efficiently reduced LPS-induced NOS2 expression in microglia (**Fig.3d**). Collectively, these data demonstrate that inhibition of caspase 3 contributes to the microglial tumor-supportive activation state.

Glioma NOS2 contributes to S-nitrosylation of caspase 3

Our next step was to elucidate how caspase 3 inhibition can be achieved in microglia cells. Repression of caspase 3 activity via the potential down-regulation of the basal enzymatic activity of its upstream regulator, caspase 8, could already be excluded as LETDase activity was not found to be significantly affected during glioma-induced microglia activation (**Supplementary Fig.1b**). The mRNA expression levels for these

two caspases could not explain the observed reduction of caspase 3 activity in microglia upon coculture with glioma cells (**Supplementary Fig.4a,b**). Previous studies support a tumor-promoting role for endogenous nitric oxide (NO) in malignant glioma[18, 19]. Of particular interest for the current investigations, NO produced by NOS, has long been recognized as instrumental in the regulation of capase-3 activation[20, 21]. Indeed, caspase 3 zymogen is subject to reversible inhibitory S-nitrosylation at its catalytic Cys^{163} active site, thereby regulating its enzymatic activity (we hereafter refer to S-nitrosylated procaspase 3 as SNO-procaspase-3)[22, 23]. In agreement with the probable involvement of NOS-produced NO in the glioma-induced repression of microglial caspase 3 activity, treatment with L-NAME, a pan-NOS inhibitor, or carboxy-PTIO, a NO scavenger, prevented effectively the decrease in DEVDase activity observed in BV2 and primary mouse microglia upon coculture with glioma (**Fig.4a**). Furthermore, using the biotin switch method[24], we quantified the extent of S-nitrosylation of microglial procaspase 3 under microglia-glioma segregated coculture as compared to microglia monoculture conditions. In fact, increased expression of SNO-procaspase 3 was observed in microglia cells upon coculture with glioma cells (**Fig.4b**). Using *in situ* proximity ligation assay (PLA) to identify protein carrying SNO-Cys residues[25], increased S-nitrosocysteine post-translational modification of procaspase 3 was confirmed in microglia under segregated coculture condition with glioma cells (**Fig.4c**).

Finally, we sought to identify the source of NO used for caspase 3 S-nitrosylation. NOS2, also known as inducible NOS, produces NO in response to various stimuli. Use of a selective NOS2 inhibitor, 1400W, abrogated glioma-induced repression of microglial DEVDase activity (**Fig.4a**). In this glioma-microglia cell communication system two potential cell origins for NO production can be envisaged. However, an almost complete abrogation of *Nos2* mRNA expression was observed in BV2 microglia upon 6 hours coculture with C6 glioma cells, suggesting that NO should originate from the C6 glioma cells (**Fig.2d**). In contrast to the glioma effect on microglia NOS2 expression, we found that microglia cells promoted *Nos2* mRNA expression in glioma cells upon coculture

(**Fig.4d**). Pooled siRNA targeting *Nos2* expression was found to negatively affect the ability of C6 glioma cells to repress microglial caspase 3 like activity (**Fig.4e,f**). Thus, NOS2 activity originating from the glioma cells appeared to act as an initiating stimulus in the control of microglial caspase 3 activity.

Trx2 activity prevents S-nitrosylation of caspase 3

The thioredoxin (Trx) family of small redox proteins has been reported to affect the nitrosylation status of caspase-3[22, 23, 26]. Mammals have two classical Trxs, cytosolic or nuclear thioredoxin-1 (Trx1) and mitochondrial thioredoxin 2 (Trx2), both of which have been identified as major protein denitrosylases. Under certain conditions, Trx1 may also catalyze *trans-S*-nitrosylation of proteins through mechanisms involving its Cys^{69} or Cys^{73} residues, which are not present in Trx2[26]. We therefore decided to assess the respective roles of the Trxs in regulating the nitrosylation status of caspase-3, and thereby its proteolytic activity, by selectively knocking down endogenous Trx1 or Trx2 in BV2 microglia cells (**Supplementary Fig.5a**). BV2 microglia cells transfected with siRNAs pool specifically targeting Trx1, but not Trx2, exhibited higher caspase 3 like activity as compared to siControl monoculture. However, when BV2 microglia cells were transfected with siRNA specifically targeting Trx2, but not Trx1, glioma cells did not repress caspase 3 like activity in microglia, proportionally, as effectively as compared to their respective monocultures (**Fig.5a**). The poor efficacy of Trx1 inhibition in counteracting glioma-induced microglial DEVDase activity decrease was further validated with the use of a selective Trx1 inhibitor, PX-12 (**Supplementary Fig.5b**). In addition, upon coculture with glioma cells, increased S-nitrosylation of Trx2 (**Supplementary Fig.5c**) but decreased mitochondrial Trx activity, accounting for the activity of the mitochondrial-specific Trx2 (**Supplementary Fig.5d**) could be observed in microglia cells. Overall, the glioma's influence over microglia cells appeared to be associated with an inhibition of the Trx redox system (with reduction of both Thioredoxin and Thioredoxin Reductase activities) (**Supplementary Fig.5d,e**). Importantly, we found that reducing microglial Trx2 expression recapitulated the effect of glioma cells stimulation on SNO-procaspase 3

232 expression in microglia, suggesting that regulation of Trx2 accounts for the observed
233 phenomenon (**Fig.5b**).

234 Since Trx2 is a mitochondria-specific thioredoxin, and procaspase 3 can be found both in
235 the cytosolic and mitochondrial cell compartments, we decided to determine the
236 subcellular compartment(s) where glioma-induced microglial SNO-procaspase 3 induction
237 takes place. Subcellular fractionation experiments revealed that procaspase 3 could be
238 found in both cytosolic and mitochondrial fractions of microglia cells, while cleaved
239 caspase 3 was only detected in the cytosolic fraction (**Fig.5c**), which also accounted for
240 most of the DEVDase activity in the cell (**Fig.5d**). In addition, upon coculture with glioma
241 cells, decreased cleaved caspase 3 levels and associated caspase 3 like activity was
242 observed in the cytosol of microglia cells (**Fig.5c,d**). Finally, these experiments also
243 showed that increased S-nitrosylation of procaspase 3 occurred primarily in the
244 mitochondria of microglia cells upon stimulation by glioma cells (**Fig.5e**). Thus, these
245 experiments indicate that inhibition of Trx2-mediated denitrosylation of mitochondrial
246 SNO-procaspase 3 is part of the microglial activation pathway initiated by glioma cancer
247 cells.

248 **Glioma NOS2 inhibits microglial caspase 3 activity**

249 Collectively, these data let us propose a microglia-glioma cell-cell communication
250 signaling pathway, wherein NO produced by NOS2 in glioma cells leads to an S-
251 nitrosylation-dependent inhibition of Trx2 activity in microglia, which in turn results in
252 increased S-nitrosylation and inhibition of caspase-3, an event which promotes the
253 tumor-supportive phenotype of microglia. To validate this signaling pathway *in vivo*, we
254 inhibited the most upstream component, NOS2 in glioma cells, and assessed its biological
255 consequences on tumor growth and microglia recruitment *in vivo*. Viral delivery of small
256 hairpin RNA (shRNA) targeting *Nos2* was used for establishment of GL261-derivatives
257 with stable knockdown of NOS2 (**Fig.6a**). *Nos2* shRNA expressing GL261 glioma cells
258 exhibited a reduced ability to reduce microglial caspase 3 like activity, as compared to

control shRNA expressing cells (**Fig.6b**). GFP-GL261 cells expressing a control shRNA or a *Nos2* shRNA were injected into young C57/BL6/J mice brains[12]. Immunohistochemical analysis of brain tissues after 1 and 2 weeks post-transplantation, revealed a marked reduction in tumor growth in mice injected with *Nos2* shRNA expressing GFP-GL261 cells, as compared to control shRNA expressing GFP-GL261 cells (**Fig.6c-f**). The accumulation of Iba1-positive amoeboid (activated) microglia within and around the implanted glioma was found to be considerably reduced in mice injected with *Nos2* shRNA expressing GFP-GL261 cells (**Fig.6c-f**). These *in vivo* experiments suggest that glioma's NOS2 activity contributes to the recruitment of microglia towards the tumor.

Microglial caspase 3 depletion supports glioma tumor growth

Microglia are characterized by prominent expression of the chemokine receptor CX3CR1. Due to the cellular kinetics of blood cell replenishment versus microglial longevity, mice containing a Cre recombinase fused to the ligand-binding domain of T2 estrogen receptor variant (ERT2) under the control of the *Cx3cr1* promoter/enhancer elements, *i.e.* *Cx3cr1*^{CreERT2} mice, allows the generation, in response to tamoxifen treatment, of animals that harbor specific genetic manipulations restricted to microglia[27, 28]. In order to provide direct evidence that just microglia-related caspase 3 is important for glioma expansion in vivo, *Casp3*$^{flox/flox}$ mice bearing the *Casp3* allele floxed at exon 2 (Ref. 29) were crossed with *Cx3cr1*^{CreERT2} mice (**Fig.7a**). *Casp3* deletion was first evaluated 7 days after tamoxifen treatment, used to induce the specific deletion of *Casp3* in microglia cells. Microglia were isolated by immunomagnetic cell sorting and qPCR analysis demonstrated a high efficiency for microglial *Casp3* gene deletion (>75%) in *Casp3*$^{flox/flox}$*Cx3cr1*^{CreERT2} [Caspase 3 deficient microglia] mice brains as compared to *Casp3*$^{flox/flox}$ [used as control] mice brains (**Fig.7a**). It could be argued that microglia lacking caspase 3 could be replaced by newly-generated microglial cells expressing this critical caspase. However, identical analysis performed at 6 months post-tamoxifen treatment, revealed sustained *Casp3* gene deletion in microglia cell population (**Supplementary Fig.6a**) in agreement with the reported long-lived nature and limited self-renewal of microglia[30]. Analysis of

striatum and cortex brain regions did not reveal any increase in the microglia cell populations in *Casp3*$^{flox/flox}$*Cx3cr1*^{CreERT2} as compared to *Casp3*$^{flox/flox}$ mice brains (**Supplementary Fig.6b-d**). When GFP-GL261 cells were injected into *Casp3*$^{flox/flox}$ and *Casp3*$^{flox/flox}$*Cx3cr1*^{CreERT2} young mice brains, immunohistochemical analysis of brain tissues after 1 and 2 weeks post-transplantation, revealed a marked increase in the tumor size upon conditional depletion of caspase 3 in microglia, as compared to control (**Fig.7b-e**). In summary, specific ablation of microglial caspase 3 affects positively their tumor-supporting function and thereby glioma expansion *in vivo*. Collectively these data show that glioma cells induce microglial caspase 3 S-nitrosylation, altering its activity and influencing the tumor-promoting properties of microglia (**Supplementary Fig.7a** and **b)**.

Discussion

Malignant gliomas are highly aggressive primary brain tumors with limited therapeutic options, and a dismal prognosis for patients[31]. Gliomas are heterogeneous with respect to the composition of bona fide tumors cells and with respect to a range of intermingling non-neoplastic cells which also play a vital role in controlling the course of the pathology. In fact, the pathologic incident of a brain tumor induces the accumulation of myeloid cells, especially at the tumor edge, which can constitute up to one third of the glioma tumor mass[32]. These are composed of microglia, the resident immune cells of the central nervous system (CNS), and additionally macrophages derived from outside the CNS. The respective impact of brain resident microglia versus macrophages originating from extra-CNS sources on tumor progression has been subject to intense debate[2]. However, studies using head-protected irradiation chimeras demonstrated in glioma mouse models that resident microglia represent the main and early source of myeloid cells within glioma. Peripheral macrophages were only found to infiltrate at the late stage of tumor growth and represent ~25% of all myeloid cells[12, 33]. Selective depletion of microglia from *ex vivo* cultured organotypic brain slices or murine *in vivo* models further illustrated the essential role for microglia *per se* in controlling glioma growth and invasion or even

tumor angiogenesis[3, 4, 33, 34]. There is a growing recognition of the functions of microglia in glioma maintenance and progression[2]. During the course of disease, microglia undergo functional changes towards a tumor-supportive phenotype. However, the underlying molecular mechanism used by glioma cells to transform the microglial cell population remains elusive.

Previous studies support a tumor-promoting role for endogenous NO and NO synthases in malignant glioma[18, 19, 35]. Evaluation of data contained in the Repository of Molecular Brain Neoplasia Data (REMBRANDT) database revealed that high NOS2 expression correlates with decreased survival in glioma patients. Furthermore, it has been demonstrated that NOS2 inhibition, in particular in the glioma stem cell population, can slow down glioma growth in a murine glioma model[19]. We provide compelling evidence that glioma-derived NO is critical in the control of microglia activation, thus exposing a completely novel role for NOS2 in glioma. *In vivo*, repressing glioma NOS2 expression resulted in reduced accumulation of microglia within and around implanted glioma which correlated with decreased tumor expansion. We report that glioma's NOS2 contributes to the repression of caspase 3 function in the microglia, via S-nitrosylation of the protease. We also provide evidence that inhibition of Trx2-mediated denitrosylation activity accounts for the observed increase in SNO-procaspase 3.

Even if so-called killer caspases, such as caspase 3, are seen as the usual suspect in the death of cells, the opinion that the apoptotic caspases are more than just killers is supported by numerous studies. In the brain, activation of caspase 3 can occur in various cell types as part of multiple non-apoptotic, essential cell functions[36-38]. For microglia, it has been previously reported that controlled caspase 3 activation contributes to the activation of these cells toward the pro-inflammatory phenotype in the absence of death[7, 9, 39]. Here, we report that glioma-induced microglia conversion is coupled to a reduction of basal microglial caspase 3 activity, increased S-nitrosylation of mitochondria-associated caspase 3 through inhibition of Trx2 activity, and demonstrate that caspase 3 inhibition regulates microglial tumor-supporting function. Finally, to provide direct

evidence that just microglia-related caspase 3 is important for glioma expansion *in vivo*, we took advantage of floxed *Casp3* crossed with *Cx3cr1*^{CreERT2} mice, which allowed the generation, in response to tamoxifen treatment, of animals that harbor specific genetic manipulations restricted to microglia[27, 28]. When glioma cells were injected into *Casp3*$^{flox/flox}$ *Cx3cr1*^{CreERT2} mice, a marked increase in tumor size was observed 1 and 2 weeks post-transplantation as compared to *Casp3*$^{flox/flox}$ mice brains used as control.

We have therefore uncovered a novel role for caspase 3 in the control of microglia activation in the context of glioma expansion. We found that inhibition of basal caspase 3 activity in microglia is associated with the polarization of these cells toward a tumor-supportive phenotype. Despite the importance of microglia in the maintenance of CNS homeostasis and the pathogenesis of neurodegenerative diseases and brain tumors, the molecular mechanisms behind their polarization toward selective phenotypes remain unclear. Our investigations uncover the pivotal role for caspase 3 in the regulation of microglia biology. Caspase 3 may work as a rheostat which controls microglial cell fate in response to diverse stimuli, where elevated activity of the protease leads to cell death, but low activity and reduced basal caspase 3 activity regulate, respectively, the pro-inflammatory and the tumor-supporting microglial activation states. Thus, caspase 3 may serve as a key determinant for microglial polarization, and suggest that its modulation could have therapeutic benefits to combat brain diseases where microglia play a role in pathogenesis.

Accessions code

Gene array data has been deposited in the Gene Expression Omnibus (GEO, accession number GSE84772).

Acknowledgments

We thank for providing us with reagents, G. Brown (University of Cambridge; BV2 cell line), R. Glass (Max Delbruck Center; GL261 cell line); O. Hermanson (Karolinska

Institutet; C6 cell line), M. Nister (Karolinska Institutet; U-251MG, U-343MG, U-373MG, U-87MG, and U-1241MG cell lines) and M. Schultzberg (Karolinska Institutet, CHME3 cell line) and for technical support the CLICK Imaging Facility supported by the Knut and Alice Wallenberg Foundation. X.S. and A.M.O. are supported by a doctoral fellowship from the Karolinska Institutet Foundations and the Swedish Childhood Cancer Foundation, respectively; M.A.B. is supported by a postdoctoral fellowship from Swedish Research Council. This work has been supported by grants from the Swedish Research Council (to B.J.), Swedish Childhood Cancer Foundation (to B.J. and K.B.), Strategic Research Programme in Cancer (StratCan)(to B.J.) and Neuroscience (StratNeuro)(to K.B.), Swedish Cancer Foundation (to B.J.), Spanish MINECO/FEDER/UE (to J.L.V.), Swedish Cancer Society (to B.J.), Swedish Brain Foundation (to B.J.), governmental grants for researchers working in healthcare (ALF)(to K.B.), and Karolinska Institutet Foundations (to B.J.).

Author Contributions

X.S. and M.A.B. performed all the experiments except otherwise noted. A.M.O., A.C-J., J.V. and K.B. contributed with *in vivo* analyses. V.R., U.N. and J.H participated with the human xenograft mouse model. J.F. contributed with the biotin switch method analysis. M.A. and A.Ö. contributed with generation of shRNA NOS2 stable transfectant. S.K. and A.B. contributed with primary microglial cell culture preparation. A.R. and R.A.F. provided the *Casp3* floxed mice. D.S. and J.R. participated with some of coculture experiments. E.K. was involved in study design. X.S., M.A.B. and B.J. designed the study, analyzed and interpreted the data. M.A.B. and B.J. wrote the first draft of the manuscript. All authors discussed the results and commented on or edited the manuscript.

Competing Financial Interests

The authors declare no competing financial interests.

References

1. Saijo, K. & Glass, C.K. Microglial cell origin and phenotypes in health and disease. *Nature reviews. Immunology* **11**, 775-787 (2011).
2. Hambardzumyan, D., Gutmann, D.H. & Kettenmann, H. The role of microglia and macrophages in glioma maintenance and progression. *Nat Neurosci* **19**, 20-27 (2016).
3. Markovic, D.S., Glass, R., Synowitz, M., Rooijen, N. & Kettenmann, H. Microglia stimulate the invasiveness of glioma cells by increasing the activity of metalloprotease-2. *Journal of neuropathology and experimental neurology* **64**, 754-762 (2005).
4. Markovic, D.S. *et al.* Gliomas induce and exploit microglial MT1-MMP expression for tumor expansion. *Proceedings of the National Academy of Sciences of the United States of America* **106**, 12530-12535 (2009).
5. Pyonteck, S.M. *et al.* CSF-1R inhibition alters macrophage polarization and blocks glioma progression. *Nat Med* **19**, 1264-1272 (2013).
6. Sarkar, S. *et al.* Therapeutic activation of macrophages and microglia to suppress brain tumor-initiating cells. *Nat Neurosci* **17**, 46-55 (2014).
7. Burguillos, M.A. *et al.* Caspase signalling controls microglia activation and neurotoxicity. *Nature* **472**, 319-324 (2011).
8. Han, Z., Hendrickson, E.A., Bremner, T.A. & Wyche, J.H. A sequential two-step mechanism for the production of the mature p17:p12 form of caspase 3 in vitro. *The Journal of biological chemistry* **272**, 13432-13436 (1997).
9. Kavanagh, E., Rodhe, J., Burguillos, M.A., Venero, J.L. & Joseph, B. Regulation of caspase 3 processing by cIAP2 controls the switch between pro-inflammatory activation and cell death in microglia. *Cell death & disease* **5**, e1565 (2014).
10. Maes, W. & Van Gool, S.W. Experimental immunotherapy for malignant glioma: lessons from two decades of research in the GL261 model. *Cancer immunology, immunotherapy : CII* **60**, 153-160 (2011).
11. Oh, T. *et al.* Immunocompetent murine models for the study of glioblastoma immunotherapy. *Journal of translational medicine* **12**, 107 (2014).
12. Muller, A., Brandenburg, S., Turkowski, K., Muller, S. & Vajkoczy, P. Resident microglia, and not peripheral macrophages, are the main source of brain tumor mononuclear cells. *International journal of cancer. Journal international du cancer* **137**, 278-288 (2015).
13. Dvorak, H.F. Tumors: wounds that do not heal. Similarities between tumor stroma generation and wound healing. *N Engl J Med* **315**, 1650-1659 (1986).
14. Wang, H. *et al.* Targeting interleukin 6 signaling suppresses glioma stem cell survival and tumor growth. *Stem cells (Dayton, Ohio)* **27**, 2393-2404 (2009).
15. Zhang, J. *et al.* A dialog between glioma and microglia that promotes tumor invasiveness through the CCL2/CCR2/interleukin-6 axis. *Carcinogenesis* **33**, 312-319 (2012).
16. Voisin, P. *et al.* Microglia in close vicinity of glioma cells: correlation between phenotype and metabolic alterations. *Frontiers in neuroenergetics* **2**, 131 (2010).
17. Zhai, H., Heppner, F.L. & Tsirka, S.E. Microglia/macrophages promote glioma progression. *Glia* **59**, 472-485 (2011).
18. Badn, W. & Siesjo, P. The dual role of nitric oxide in glioma. *Current pharmaceutical design* **16**, 428-430 (2010).
19. Eyler, C.E. *et al.* Glioma stem cell proliferation and tumor growth are promoted by nitric oxide synthase-2. *Cell* **146**, 53-66 (2011).
20. Melino, G. *et al.* S-nitrosylation regulates apoptosis. *Nature* **388**, 432-433 (1997).
21. Li, J., Billiar, T.R., Talanian, R.V. & Kim, Y.M. Nitric oxide reversibly inhibits seven members of the caspase family via S-nitrosylation. *Biochemical and biophysical research communications* **240**, 419-424 (1997).
22. Mitchell, D.A. & Marletta, M.A. le (2015).

34. Sliwa, M. *et al.* The invasion promoting effect of microglia on glioblastoma cells is inhibited by cyclosporin A. *Brain* **130**, 476-489 (2007).
35. Charles, N. *et al.* Perivascular nitric oxide activates notch signaling and promotes stem-like character in PDGF-induced glioma cells. *Cell Stem Cell* **6**, 141-152 (2010).
36. Venero, J.L., Burguillos, M.A., Brundin, P. & Joseph, B. The executioners sing a new song: killer caspases activate microglia. *Cell death and differentiation* **18**, 1679-1691 (2011).
37. Hyman, B.T. & Yuan, J. Apoptotic and non-apoptotic roles of caspases in neuronal physiology and pathophysiology. *Nat Rev Neurosci* **13**, 395-406 (2012).
38. Wang, J.Y. & Luo, Z.G. Non-apoptotic role of caspase 3 in synapse refinement. *Neuroscience bulletin* **30**, 667-670 (2014).
39. Burguillos, M.A. *et al.* Microglia-Secreted Galectin-3 Acts as a Toll-like Receptor 4 Ligand and Contributes to Microglial Activation. *Cell Rep* **10**, 1626-1638 (2015).

Figure Legends

Figure 1 | Glioma cells promote a decrease of basal caspase 3 activity in microglia cells. (**a**-**d**) DEVDase activity in BV2 (**a**,**b**), CHME3 (**c**), or mouse or human primary (**d**) microglia cultured for 6 h (**a-**left,**b**,**c**,**d**) or 24 h (**a**-right) as monoculture (–) or with various glioma cells (horizontal axis) as segregated (**a**,**c**,**d**) or joint (**b**) cocultures; Results are presented relative to those of each monoculture, set as 1. (**e**) DEVDase activity in indicated microglia cultured in control- or C6 glioma conditioned-medium; results are presented relative to those of control-medium condition, set as 1. (**f**,**g**) Immunoblot analysis of cleaved caspase 3 upon immunoprecipitation (IP) (**f**) and procaspase 3 and β-actin (**g**) in BV2 microglia grown as monoculture or with C6 as segregated coculture. In panel **f**, inflammogen LPS, death stimulus STS treatments and IgG were used controls. (**h**) Confocal microscopy of tumor formed in mouse brain, 1 week post-injection of GFP-GL261 cells and immunostaining for cleaved caspase 3 and Iba1 (microglia marker) and Hoechst nuclear counterstain. Dashed white line delimits the border of formed tumor; Scale bar, 20μm. (**i**) 2.5D analysis of section depicted in **h**. (**J**) Quantification of microglial cleaved caspase 3 signal intensity at the border or inside tumor at 1 week (n=40 cells) and 2 weeks (n=30 cells). *P< 0.05; **P< 0.01; ***P< 0.001 and ****P< 0.0001 (two-tailed Student's t-test). Data are from at least three independent experiments (n=6 (**a**,**d**(mouse)), 4 (**b**,**c**,**g-**bottom) or 3 (**d**(human),**e**); mean and s.d.) or representative of at least three experiments with similar results (n=3(**f**), 4(**g-**top)) or one independent experiment (n=6 mice (**h**,**i**), 40 cells (**j** 1 week) or 30 cells (**j** 2 weeks)).

Figure 2 | Knockdown of caspase 3 promotes the microglial tumor-supportive phenotype. (**a**,**b**) Immunoblot analysis of procaspase 3 and β-actin (**a**) and DEVDase activity (**b**) in BV2 microglia transfected with indicated siRNA; results are presented relative to those of Ctrl siRNA transfected BV2 cells, set as 1. (**c, d**) Quantification of mRNA expression of the indicated genes (horizontal axis) (**c**, gene array and **d**, qPCR analysis) in BV2 microglia transfected with indicated siRNA and grown as monoculture or

with C6 cells as segregated coculture (key); results are presented relative to those of Ctrl siRNA transfected BV2 monoculture, set as 1. (**e**) Quantification of C6 glioma cells migration (left histogram) and invasion (right histogram) capabilities in transwell assays placing BV2 microglia transfected with the indicated siRNA in the lower compartment; results are presented relative to those of C6 cells exposed to siCtrl BV2, set as 1. *P< 0.05; **P< 0.01; ***P< 0.001 and ****P< 0.0001 (two-tailed Student's t-test (**a, b, d**), one-way ANOVA with Bonferroni correction (**e**)). Data are from at least three independent experiments (n=3 (**a-**bottom,**b**), 4 (**d**,**e**); mean and s.d., except **d** mean and s.e.m.) or representative of three experiments with similar results (**a-**top**, c**).

Figure 3 | C6 glioma cells counteract LPS-induced DEVDase activity and NOS2 expression in BV2 microglia cells. (**a**,**b**) DEVDase activity (**a**) or LETDase activity (**b**) in BV2 microglia pre-treated with various concentration of LPS (horizontal axis, in μg/ml) for 24 hours prior to segregated coculture with C6 glioma cells (horizontal axis); results are presented relative to those of untreated BV2 monoculture, set as 1. (**c**) Immunoblot analysis of cleaved caspase 3 upon immunoprecipitation (IP) following experimental set up described in panel **a**. IgG was used as experimental control. (**d**) Immunoblot analysis (top) of NOS2 and β-actin in BV2 microglia following experimental set up described in panel **a**. Bottom, quantification of the results at top; presented relative to those of LPS-treated BV2 monoculture, set as 1. ns, not significant, *P< 0.05; **P< 0.01; ***P< 0.001 and ****P< 0.0001 (two-tailed Student's t-test (**a**,**b**,**d**)). Data are from at least three independent experiments (n=4 (**a**,**b**), 3 (**d-**bottom); mean and s.d.) or representative of three experiments with similar results (**c**,**d-**top).

Figure 4 | Glioma NOS2 contributes to S-nitrosylation of microglial caspase-3. (**a**) DEVDase activity in BV2 (left) or primary mouse (right) microglia grown as monoculture or with C6 glioma cells as segregated coculture and exposed to indicated treatments (horizontal axis) (**b**) Immunoblot analysis (left) of S-nitrosylated procaspase 3 (BS, biotin switch assay) and procaspase 3 (lysate) and quantification of S-nitrosylation of procaspase 3 (right) in BV2 microglia grown as monoculture or with C6 cells as

segregated coculture. Minus biotin or ascorbate and pre-photolysis were used as controls. (**c**) *In situ* proximity-ligation assay (left) and quantification (right) of nitrosocysteine-procaspase 3 interactions in BV2 microglia grown as monoculture or with C6 cells as segregated coculture. $HgCl_2$ treatment was used as control. In panel **a**-**c** results are presented relative to those of BV2 monoculture, set as 1. (**d**,**e**) Quantification of *Nos2* mRNA in C6 glioma cells grown as monoculture or with BV2 microglia as segregated coculture (**d**) or in BV2 microglia (left) or C6 cells (right) transfected with indicated siRNA (horizontal axis) (**e**); Quantification of *Nos2* mRNA results are presented relative to those of C6 monoculture (**d**) or siCtrl transfected cells (**e**), set as 1. ns, not significant; **P*< 0.05; ***P*< 0.01 (two-tailed Student's *t*-test (**a-e**), one-way ANOVA with Bonferroni correction (**f**)). Data are from at least three independent experiments (*n*=3 (**a**(BV2),**b**-right,**d**,**e**,**f**), 5 (**c-**right) or 6 (**a**(primary); mean and s.d. in **a**,**b**,**d**,**e**,**f**; mean and s.e.m. in **c**) or are representative of at least three experiments with similar results (*n*=3 (**b-**left), 5 (**c-**left)).

Figure 5 | Inhibition of microglial Trx2 activity promotes S-nitrosylation of mitochondrial caspase-3. (**a**) DEVDase activity in BV2 microglia transfected with indicated siRNA grown as monoculture or with C6 cells as segregated coculture; results are presented relative to those of Ctrl siRNA transfected BV2 monoculture, set as 1. (**b**) Immunoblot analysis (top) of S-nitrosylated procaspase 3 (BS, biotin switch assay) and procaspase 3 (lysate) and quantification of S-nitrosylation of procaspase 3 (bottom) following experimental setup and data presentation as in panel a. (**c**) Immunoblot analysis of cleaved caspase 3 (IP) and procaspase-3, GAPDH for cytosolic fraction, and VDAC for mitochondrial fraction (lysate) in the indicated subcellular fractions of BV2 microglia grown as monoculture or with C6 cells as segregated coculture. (**d**) DEVDase activity in subcellular fractions as described in panel **c**; results are presented relative to those of cytosol fraction of BV2 monoculture, set as 1. (**e**) Immunoblot analysis (top) of S-nitrosylated procaspase 3 (BS) and procaspase-3, GAPDH and VDAC (lysate) and quantification of S-nitrosylation of procaspase 3 (bottom) in the indicated subcellular

fractions of BV2 grown as monoculture or with C6 cells as segregated coculture. In bottom part results are presented as in panel **d**. ns, not significant; *P< 0.05; **P< 0.01 (one-way ANOVA with Bonferroni correction (**a, b**), two-tailed Student's t-test (**d, e**)). Data are from at least three independent experiments (n=3 (**a**,**b-**bottom), 4 (**d**,**e-**bottom); mean and s.d. in **a**,**b**; mean and s.e.m. in **d**,**e**) or are representative of at least three experiments with similar results (n=3 (**b**-top,**c**), 4 (**e-**top)).

Figure 6 | Inhibition of glioma NOS2 restricts inhibition of microglial caspase 3 activity, microglia recruitment and tumor growth. (**a**) Quantification of *Nos2* mRNA in GL261 cells transfected with indicated shRNA (key)*;* results are presented relative to those of shCtrl transfected GL261 cells, set as 1. (**b**) DEVDase activity in BV2 microglia grown as monoculture or with GL261 cells transfected with indicated shRNA as segregated coculture; results are presented relative to those of BV2 monoculture, set as 1. (**c,d**) Confocal microscopy of tumors formed in mice, one week (**c**) and two weeks (**d**) post-injection of shCtrl-expressing or shNos2-expressing GFP-GL261 cells together with an immunostaining for Iba1 (microglia marker) and Hoechst nuclear counterstain; Scale bars, 50µm in **c** and 200µm in **d**. (**e**,**f**) Quantification of tumor size (left) and microglia occupancy (right) in mice at 1 week (**e**) and two weeks (**f**) following procedure describe in **c**,**d**. ns, not significant; *P< 0.05; ***P< 0.001 (two-tailed Student's t-test, expect for **b** one-way ANOVA with Bonferroni correction). Data are from at least one independent experiments (n=4 (**a**), 5 (**b**) or 1 (n=6 mice per group (**e**), 5 mice per group (**f**)); mean and s.d.) or are representative of one independent experiment (n=6 mice per group (**c**), 5 mice per group (**d**)).

Figure 7 | Depletion of microglial procaspase 3 promotes glioma tumor growth. (**a**) Scheme illustrating the tamoxifen-inducible *Casp3*$^{flox/flox}$*Cx3cr1*^{CreERT2} mice system used to generate deletion of caspase 3 in microglia cells (left) and genotyping of *Casp3*$^{flox/flox}$ and *Casp3*$^{flox/flox}$*Cx3cr1*^{CreERT2} mice using DNA from fingers or microglia as indicated (right). (**b**,**c**) Confocal microscopy of tumor formed in *Casp3*$^{flox/flox}$*Cx3cr1*^{CreERT2} and Casp3$^{flox/flox}$ mice, (**b**) 1 week and (**c**) 2 weeks post-injection of GFP-GL261 glioma

cells using Hoechst as nuclear counterstain; Scale bars, 50µm in **b** and 100µm in **c**. (**d**) Quantification of tumor size and (**e**) microglia occupancy in *Casp3*$^{flox/flox}$*Cx3cr1*^{CreERT2} and Casp3$^{flox/flox}$ mice at 1 week and 2 weeks post-injection of GFP-GL261 glioma cells. ns, not significant; *P< 0.05 (two-tailed Student's t-test). Data are from one independent experiment (n=4 mice per genotype (**d**,**e**(1 week)), 5 mice per genotype (**d**,**e**(2 weeks)); mean and s.e.m.) or are representative of one independent experiment (n=4 mice per genotype (**b**), 5 mice per genotype (**c**)).

Online Methods

Reagents

Lipopolysccharide from *Escherichia coli*, serotype 026:B6, staurosposrine and carboxy-PTIO from Sigma-Aldrich, 1400W dihydrochloride, L-NAME hydrochloride and 2-[(1-Methylpropyl)dithio]-1H-imidazole from TOCRIS Bioscience were used in this study.

Cell lines culture and transfection

BV2 (gift of G. Brown, University of Cambridge) and CHME3 (from originator M. Tardieu, Paris-Sud University) microglial cell lines and C6, U-87MG (purchased from ATCC), U-251MG, U-343MG, U-373MG, U-1241MG (were stock from B. Westermark originator's laboratory, Uppsala University), and GFP-GL261 (gift of R. Glass, Max Delbruck Center) glioma cell lines, regularly tested with Venor^{TM}GeM mycoplasma detection kit (Minerva Biolabs), were cultured as previously described[7, 12]. A transwell system as depicted in **Supplementary Fig.1a** was used for segregated cocultures. Transfection of BV2 and C6 cells was carried out with Lipofectamine® 2000 (Invitrogen) and Amaxa® cell line nucleofector kit V (Lonza) respectively. Non-targeting control, caspase-3, Trx1, Trx2 and NOS2 ON-TARGET plus SMARTpools siRNAs, whom sequences can be found in the **Supplementary Table 1**, were obtained from Dharmacon.

Human primary microglial cells

Primary human microglial cells were purchased from ScienCell Research Laboratories (Cat. #1900) and cultured in a humidified incubator with 5% CO_2 at 37 °C and maintained in DMEM/F12 medium containing 10% FBS, human M-CSF (10ng/ml; R&D systems) and gentamicin (20 µg/ml; Gibco BRL).

Mouse primary microglial cells

All protocols involving animals were approved by the Regional Animal Research Ethical Board, Stockholm, Sweden (Ethical permit N295/12 and N296/12), following proceedings described in European Union legislation. Primary mouse microglial cells were prepared from postnatal P1-2 C57BL/6/J mouse brain following previously described protocol[40].

Postnatal P1-2 C57BL/6/J mice were euthanized and brains were carefully dissected removing all the meninges and the cortices were washed in ice-cold Ca^{2+}- and Mg^{2+}-free Hanks' buffered salt solution (HBSS; Gibco BRL). Later on they were minced, and resuspended in ice-cold HBSS. After being washed, tissues were incubated for 15 min in HBSS containing 0.125% trypsin and resuspended in DMEM/F12 medium containing 10% FBS, 1% G5 supplement (Gibco BRL), and gentamicin (20 µg/ml; Gibco BRL). Medium was replaced completely after 1 day cell seeding. 7 days after seeding, cells were subcultivated in a concentration of 0.8~1 x 10^6 cells in a 75 cm^2 flask. 2 and 4 days later, half of the medium volume was exchanged. Microglial cells were harvested from confluent astrocyte monolayers, 14 days after the initial seeding, by tapping the side of the culture flask. These microglial cells found in the medium were plated into new dishes. Experiments were performed 24 hours after the final plating.

Establishment of GL261 cells with stable knockdown of *Nos2*

Phoenix cells were transfected with vectors encoding *Nos2*-targeting shRNA or non-targeting shRNA (Origene technologies). The viral supernatant of Phoenix cells was collected 2 days after transfection. GL261 glioma cells with stable knockdown of *Nos2* (shRNA NOS2) and an empty vector control (shRNA Ctrl) (**Supplementary Table 2**) were established by incubation of GL261 cells with the viral supernatant for 5 hours and subsequent selection in puromycin-supplemented DMEM medium for 10 days. Efficient shRNA-mediated knockdown of *Nos2* in glioma cells was confirmed by qRT-PCR. Puromycin-resistant glioma mass cultures expressing shRNA Ctrl or shRNA NOS2-targeting shRNA were used for further studies.

Caspase activity assay

DEVDase and LETDase activities in microglia were measured using the Caspase-Glo®3/7 and Caspase-Glo®8 luciferase based assay (Promega) following manufacturer's instruction. Equal volume of sample and kit component were mixed onto a 96 well plate and incubated for 1 h at room temperature. The plate was analyzed using a luminometer and the value obtained was normalized with the number of cells at harvest or by protein

amount for each subcellular fractions. Caspases activities were measured at 6 hours, otherwise noted.

Immunoprecipitation and Immunoblotting

Total protein extracts were made directly in Laemmli buffer. For immunoprecipitation, cells were lysed in an IP lysis buffer (20mM Tris-HCl pH 7.5, 140mM NaCl, 1% Triton-X100, 2mM EDTA, 1mM PMSF, 10% glycerol and Protease Inhibitor Cocktail) for 15 min before sonication. Protein G Sepharose (GE healthcare) precleared total protein extracts were incubated with the cleaved caspase-3(Asp175) rabbit polyclonal antibody (**Supplementary Table 3**) in IP lysis buffer overnight at 4°C. Normal rabbit IgG was used as control. Immunocomplexes bound to protein G-Sepharose were collected by centrifugation and washed in IP wash buffer (50mM Tris-HCl, pH 7.5, 0.1% SDS, 1% NP40, 62.5mM NaCl). For immunoblot analysis, protein extracts were resolved on 12 or 15% SDS–polyacrylamide gel electrophoresis and then blotted onto nitrocellulose membrane. Membranes were blocked in 5% milk and incubated with indicated primary antibodies raised against cleaved caspase-3(Asp175), Trx2, or NOS2, overnight at 4°C, followed by incubation with the appropriate horseradish peroxidase secondary antibody (Pierce, 1:10,000) for 1h at room temperature. Immunoblot with anti-β-actin antibody was used for standardization of protein loading. Details about antibodies used in this study can be found in **Supplementary Table 3**. Bands were visualized by enhanced chemiluminescence (ECL-Plus, Pierce) following the manufacturer's protocol. Densitometry was done using ImageJ.

Subcellular fractionation

Subcellular fractions were obtained following previously described protocol[41]. Briefly, $7x10^7$ cells were resuspended in 1 ml of buffer termed A (150mM NaCl, 50mM Tris-HCl pH=8.0, 100μM EDTA, 1mM PMSF and 1x cOmplete™ Protease Inhibitor Cocktail (Roche)). Cells were homogenized though a 23G (0.6x25) syringe needle until >80% of the cells stained for trypan blue. Nuclei and unbroken cells were removed by two

successive 10 min centrifugations at 1000 g. The resulting supernatant was centrifuged at 10000 g for 30 min to isolate a pellet highly enriched in mitochondria. The mitochondrial pellets were incubated during 30 min at 4°C in a high salt buffer containing (1% NP-40, 500mM NaCl, 500mM Tris-HCl pH=8.0, 100µM EDTA, 1mM PMSF and 1x cOmplete™ Protease Inhibitor Cocktail). The insoluble material was pelleted after being centrifuged for 10 min at 4°C at 10000g.

Measurement of protein S-nitrosylation by the Biotin Switch method

Analysis of S-nitrosylation was performed according to previously described method[24] with some modifications. Upon treatment, BV2 cells were lysed in lysis buffer (50mM NaAc, 150mM NaCl, 10% NP-40 and 10% glycerol) with 1mM PMSF, 1x cOmplete™ Protease Inhibitor Cocktail (Roche) and 100µM neocuproine. Lysates were spun down in a table-top centrifuge at 21000g for 5 min, after which protein concentrations were measured with Bradford reagent (Bio-Rad). Up to 1mg of protein in lysis buffer was incubated with 50mM iodoacetic acid and 3% SDS in the dark for 30 min at room temperature with frequent vortexing. Alkylated protein was added to lysis buffer-equilibrated Zeba™ spin desalting columns (#89890, Pierce), and the buffer-exchanged protein eluates were supplemented with 1:50 dilution of 1M sodium ascorbate and 1:3 dilution of 50 mM Biotin-HPDP (#21341, Pierce), which was incubated for 1 h at room temperature while shaking. This last step reduces nitrosylated cysteine residues that will covalently bind the Biotin-HPDP. Proteins labelled with Biotin-HPDP were captured overnight with prewashed streptavidin-agarose beads (#S1638, Sigma-Aldrich) and were washed three times with the lysis buffer and run in an acrylamide gel and immunobloted against procaspase 3 or Trx2 (**Supplementary Table 3**). For validation of the biotin-switch assay, protein cell lysates were exposed to UV irradiation, which cleaves the S-NO bonds and is used as negative control, prior to biotin-switch assay[42, 43].

Measurement of protein S-nitrosylation by the *In situ* Duolink-PLA technology

Cells were seeded on coverslips and treated as indicated. Interactions between S-nitrosocysteine residues (SNO-Cys) and procaspase 3 in 4% paraformaldehyde fixed cells

were detected using the Duolink II *in situ* PLA from Olink Bioscience, following manufacturer's instructions. PLA was performed in a humidity chamber. After incubation with the supplied blocking solution, cells were incubated with the primary antibodies mouse anti-SNO-Cys and rabbit anti-procaspase 3 (**Supplementary Table 3**) in the antibody diluent medium overnight at 4°C. Cells were washed with supplied buffer A and incubated for 1 h in a humidity chamber at 37 °C with PLA probes detecting mouse or rabbit antibodies (Duolink II PLA probe anti-rabbit plus and Duolink II PLA probe anti-mouse minus diluted in the antibody diluent to a concentration of 1:5). After washing with buffer A, cells were incubated for 30 min at 37 °C with the ligation solution (Duolink II Ligation stock 1:5 and Duolink II Ligase 1:40). If the two protein targets are in close proximity, a template is formed for amplification. Detection of the amplified probe was done with the Duolink II Detection Reagents Red Kit. After repeated washing at room temperature with wash buffer B, coverslips were mounted onto slides using mounting medium containing DAPI and samples were observed using a confocal microscope. Protein–protein interaction was measured as the number of fluorescent dots/cell analyzed with Duolink Image tool. As negative control, cells were treated with 0.2% $HgCl_2$ for 30 min at room temperature prior to PLA[44].

Measurement of Trx and TrxR activities in cell lysates

To quantify the activities of Trx and TrxR in cell lysates, we used an end point assay kit (IMCO Ltd AB) based on the reduction of insulin disulfides by reduced Trx with TrxR and NADPH as ultimate electron donor.

RNA isolation, cDNA synthesis, and qPCR

RNA was isolated from 2 x 10^5 cells using the total RNA extraction kit (Qiagen). cDNA was synthesized from 1 µg RNA using Oligo dT, dNTPs, and Superscript II (Invitrogen). qPCR was performed using Sybr® Green reagents (Applied Biosystems) and primers listed in **Supplementary Table 4**. Results were calculated using delta Ct method and represented as a fold over untreated cells.

Gene expression array analysis

The mouse wound healing RT² profiler PCR array (PAMM-121Z; Qiagen) was used to profile the expression of 84 genes central to the wound healing response using manufacturer's instructions. cDNAs were synthesized from 1 µg of mRNA using RT^2 First Strand Kit from Qiagen.

Transwell migration and invasion assays

8µm-pore width transparent PET membrane inserts (Transwell, Corning) were used to measure cell migration capability. To quantify the cell invasion capability, the inserts were coated with 300µg/ml Growth Factor Reduced Matrigel® Matrix (Corning). 100µl of Matrigel® Matrix was added per insert and air-dried under sterile conditions at 37°C. C6 glioma cells were seeded on top of the insert and BV2 microglia were seeded in the lower compartment. Once the experiment was finalized, the membranes from the inserts were washed with PBS and carefully cut out with a blade. Later on, the membranes were mounted with ProLong Gold antifade reagent with DAPI (Life technologies) and the nuclei of the migrated cells were counted under fluorescent microscopy.

Generation of microglia specific *Casp3* deficient mice

Experiments were performed in accordance with the Guidelines of the European Union Council, following Spanish regulations for the use of laboratory animals and approved by the Scientific Committee of the University of Seville, Spain. *Casp3*$^{flox/flox}$ C57BL/6/J mice with the *Casp3* allele floxed at exon 2 and C57BL/6/J mice containing a Cre recombinase under the control of *Cx3cr1* promoter and enhancer elements (Jackson Laboratories, B6.129P2(Cg)-Cx3cr1tm2.1(cre/ERT)Litt/WganJ), were crossed to generate *Casp3*$^{flox/flox}$*Cre*$^{Cx3cr1+/-}$ (microglial *Casp3* KO mice) and *Casp3*$^{flox/flox}$*Cre*$^{Cx3cr1-/-}$ (control mice) (**Fig. 7a**). Deletion was induced upon tamoxifen daily treatment for four consecutive days starting at postnatal day P7. All mice (Cre+ and Cre-) were injected with tamoxifen at the following doses: P7 and P8, 50µg/pup; P9 and P10, 100µg/pup. Genotyping of the mice was done by PCR analyses of finger DNA using the following

primers for the *Casp3* floxed allele: (A) GAGCCTTCATAGGGGTGCAA, (B) GGGGAGCAGAGGGAATAAAG and (C) CATAGAATCCCAAGCCAGGA (Sigma-Aldrich), and for the *Cre* transgenes AAGACTCACGT GGACCTGCT (*Cx3cr1* Cre Common), AGGATGTTGACTTCCGAGTTG (*Cx3cr1* Cre Wild Type) and CGGTTATTC AACTTGCACCA-3´ (*Cx3cr1* Cre mutant) (Jackson Labs Technologies).

PCR and real-time PCR for assessing deletion efficiency in microglia

The effectiveness of Cre-mediated deletion of the floxed *Casp3* allele was first roughly estimated 5 days after the last tamoxifen injection by PCR in microglia isolated from the whole brain. Microglial cells were isolated from brain tissue after perfusion with ice-cold PBS, weighed, and enzymatically digested using Neural Tissue Dissociation Kit in combination with the gentleMACS Dissociator (Miltenyi Biotec), for 35 min at 37°C. Tissue debris was removed by passing the cell suspension through a 40 µm cell strainer. Further processing was performed at 4°C. After enzymatic dissociation, cells were resuspended in 30% Percoll (Sigma-Aldrich) and centrifuged for 10 minutes at 700 g. The supernatant containing the myelin was removed, and the pelleted cells were washed with HBSS, followed by immunomagnetic isolation using CD11b (Microglial) MicroBeads mouse/human (Miltenyi Biotec). After myelin removal, cells were stained with CD11b (Microglial) MicroBeads in autoMACS™Running Buffer MACS separation Buffer (Miltenyi Biotec) for 15 minutes at 4°C. $CD11b^+$ cells were separated in a magnetic field using LS columns (Miltenyi Biotec). The CD11b+ fraction was collected and used for further analyses.

For evaluation of *Casp3* gene deletion efficiency, we followed an ABC primer strategy[29] (see **Fig.7a** for locations of primers). DNA was extracted from the microglial fraction and subjected to PCR analysis using the above mentioned A, B and C primers for the *Casp3* floxed allele. DNA levels from each sample were first normalized on the basis of quantification of the *Actb* gene in the same DNA samples using CCACACCCGCCACCAGTTCG (fwd) and CCCATTCCCACCATCACACC (rev) (Sigma-Aldrich). All samples were tested in triplicate. Ct were determined by plotting normalized

fluorescent signal against cycle number, and the *Casp3* floxed and *Casp3* deleted copy number was calculated from the corresponding Ct values.

Syngeneic transplant glioma mouse model[5,32]

Experiments were performed in accordance with the Guidelines of the European Union Council, following Spanish and Swedish regulations for the use of laboratory animals and approved by the Scientific Committee of the University of Seville, Spain and the Regional Animal Research Ethical Board, Stockholm, Sweden (Ethical permits N248/13, C207/1 and N110/13). Male C57/BL6/J mice (Charles River) were housed in a 12/12 hours light/dark cycle with access to food and water *ad libitum.* Postnatal day 16-17 male pups were anesthetized with isoflurane (5% for induction and 1.5% for maintenance). An incision was made on the scalp and the skin flaps were retracted to expose the skull. Animals received an intrastriatal injection of 5 x 10^4 syngeneic G261 glioblastoma cells expressing GFP suspended in 1µl culture medium in the left hemisphere and vehicle in the right hemisphere using the following coordinates relative to bregma anterior/posterior: +0.7 mm, lateral: ±2.5 mm, ventral: -3 mm, using a 5µl ILS microsyringe. The injection was performed over 1 min and the syringe remained in the injection site for 5 min to reduce back flow, and slowly retracted over 1 min thereafter. The skin was sutured and animals were allowed to recover before they were returned to their dams. Animals were sacrificed 1 week or 2 weeks after glioma transplantation (n=6 for each time point). Animals were deeply anesthetized with sodium pentobarbital and transcardially perfused with 0.9% sodium chloride followed by fixation with 4% paraformaldehyde in 0.1M phosphate buffer (pH 7.4). Brains were then transferred to 30% sucrose in 0.1M phosphate buffer and left until they sank. 25 µm thick horizontal free-floating sections were prepared using a microtome (Leica SM2010R) and stored in cryoprotection solution at 4°C (25% glycerol, 25% ethylene glycol in 0.1M phosphate buffer) for further histological analysis.

Immunofluorescence staining

Sections were incubated in sodium citrate (pH 6.0) for 30 min at 80°C for antigen retrieval. After incubation for 1 hour in a blocking solution containing 3% normal donkey serum (Jackson ImmunoResearch Lab) and 0.1% triton X-100 to prevent non-specific binding. Later on, the sections were incubated for 48 hours with the following primary antibodies: rabbit anti-cleaved caspase-3, and goat anti-Iba-1. Sections were then incubated for 2 hours with the appropriate secondary antibodies: biotinylated donkey anti-rabbit (1:1000; Jackson ImmunoResearch Lab), Alexa-555-conjugated donkey anti-rabbit IgG (1:1000; Invitrogen), or CF-633-conjugated donkey anti-goat (1:1000; Biotium). When biotinylated antibodies were used, sections were incubated for 2 hours with CF-555-conjugated streptavidin (1:500; Biotium). Hoechst 33342 (Invitrogen) was used as a nuclear counterstain (10 min incubation).

Sections were mounted onto glass slides using the antifade reagent ProLong® Gold (Invitrogen). Samples were analysed under Zeiss LSM700 confocal laser scanning microscopy equipped with ZEN Zeiss software. Assessment of tumor size and microglial occupancy outcome were blindly analyzed by experimenter independent from the one who performed animal surgeries. Volumes in mm3 were calculated in coronal sections using the Zeiss software from the GFP-positive and Iba1-positive areas according to the Cavalieri principle using the following algorithm: $V = \Sigma A \times P \times T$, where V = total volume, ΣA = the sum of area measurements, P = the inverse of the sampling fraction, and T = the section thickness.

Intracranial human glioblastoma xenografts

Research protocols involving animal experiments were approved by the Regional Animal Research Ethical Board, Stockholm, Sweden (ethical permits C207/1 and N110/13). Female 4-to-6-week old NOD.CB17-PrkcSCID/J mice (Jackson Laboratory) were anesthetized (4% isoflurane) and received a stereotactically guided injection of 2.5×10^5 human U87 glioblastoma cells into the right striatum (2 mm lateral and 1 mm anterior to bregma at 2.5 mm depth) in 2 µL PBS. At 3 and 7 days after injection, mice were anesthetized using Avertin and perfused first with PBS and subsequently with 4%

paraformaldehyde. The brain was removed, and further fixed in 4% paraformaldehyde in a cold room overnight. After cryopreservation in 30% sucrose overnight, brains were snap-frozen and stored at −80°C until further use. Frozen brains were cut into 30 µm sections using a Leica Microtome into antifreezing medium (40% PBS, 30% ethylene glycol, 30% glycerol). Floating sections were repeatedly washed in PBS, blocked in 0.5% glycine, 0.2% Triton X-100, and 0.05% sodium azide in PBS, and incubated with primary antibody, mouse anti-human nuclei, goat anti-Iba1, rabbit anti-cleaved caspase 3 at 4°C for 48 hours (**supplementary Table 3**). Sections were then incubated for 2 hours with the secondary antibodies: biotinylated donkey anti-rabbit (1:1000; Jackson InnunoResearch Lab), Alexa-488-conjugated donkey anti-mouse IgG (1:1000; Molecular Probes, Life Technologies) and CF-633-conjugate anti-goat (1:1000; Biotium). Afterwards sections were incubated for 2 hours with CF-555-conjugated streptavidin (1:500 Biotium). Nuclei were counterstained with DAPI 1:1000 (Molecular Probes). Sections were mounted onto Superfrost Plus slides (Thermo Scientific). Samples were analysed under Zeiss LSM700 confocal laser scanning microscopy equipped with ZEN Zeiss software.

Statistical Analyses

Results were tested for statistical significance using one-way ANOVA and Bonferroni's test to correct for multiple comparisons. If two conditions were to be compared, two-tailed Student's *t*-test was used. Analyses were performed using SPSS statistical software. $P < 0.05$ was considered as statistically significant. The number of reproduced experimental repeats is described in the relevant figure legends. The investigators were not blinded to allocation during experiments and outcome assessment, except as noted above.

Methods-only-references

40. Dellacasa-Lindberg, I. *et al.* Migratory activation of primary cortical microglia upon infection with Toxoplasma gondii. *Infection and immunity* **79**, 3046-3052 (2011).

41. Mannick, J.B. *et al.* S-Nitrosylation of mitochondrial caspases. *The Journal of cell biology* **154**, 1111-1116 (2001).
42. Whalen, E.J. *et al.* Regulation of beta-adrenergic receptor signaling by S-nitrosylation of G-protein-coupled receptor kinase 2. *Cell* **129**, 511-522 (2007).
43. Forrester, M.T., Foster, M.W. & Stamler, J.S. Assessment and application of the biotin switch technique for examining protein S-nitrosylation under conditions of pharmacologically induced oxidative stress. *J Biol Chem* **282**, 13977-13983 (2007).
44. Gow, A.J. *et al.* Basal and stimulated protein S-nitrosylation in multiple cell types and tissues. *J Biol Chem* **277**, 9637-9640 (2002).

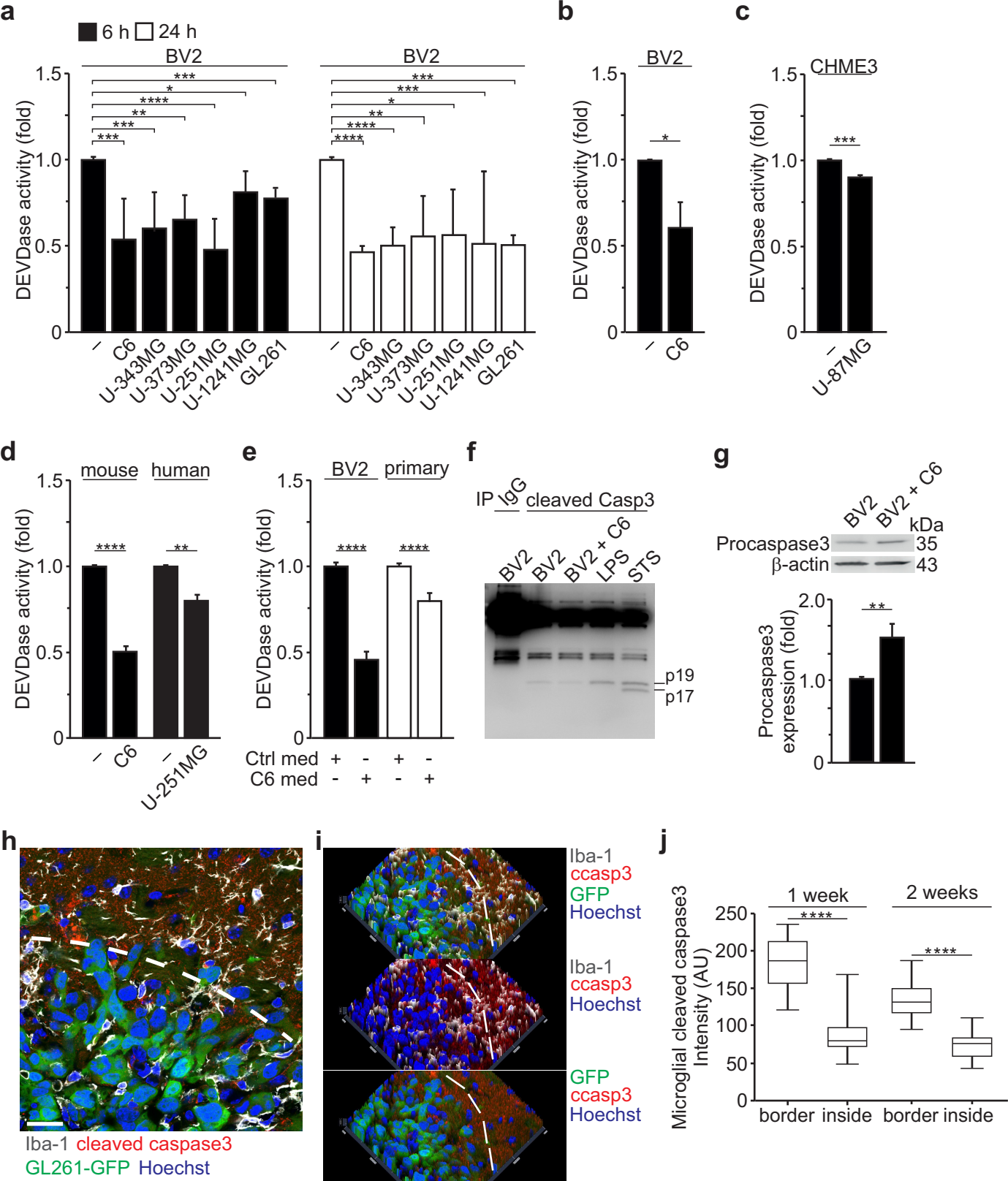
a
6 h
24 h
BV2
BV2
DEVDase activity (fold)
1.5
1.0
0.5
0
***
*
****
**
***
***
*
****
**
****
–
C6
U-343MG
U-373MG
U-251MG
U-1241MG
GL261
b
BV2
*
DEVDase activity (fold)
–
C6
c
CHME3
***
DEVDase activity (fold)
–
U-87MG
d
mouse
human
****
**
DEVDase activity (fold)
–
C6
–
U-251MG
e
BV2
primary
****
****
DEVDase activity (fold)
Ctrl med + - + -
C6 med - + - +
f
IP IgG
cleaved Casp3
BV2
BV2
BV2 + C6
LPS
STS
p19
p17
g
BV2
BV2 + C6
kDa
Procaspase3
35
β-actin
43
**
Procaspase3 expression (fold)
2.0
1.0
0
h
Iba-1 cleaved caspase3
GL261-GFP Hoechst
i
Iba-1
ccasp3
GFP
Hoechst
Iba-1
ccasp3
Hoechst
GFP
ccasp3
Hoechst
j
1 week
2 weeks
****
****
Microglial cleaved caspase3 Intensity (AU)
250
200
150
100
50
0
border
inside
border
inside

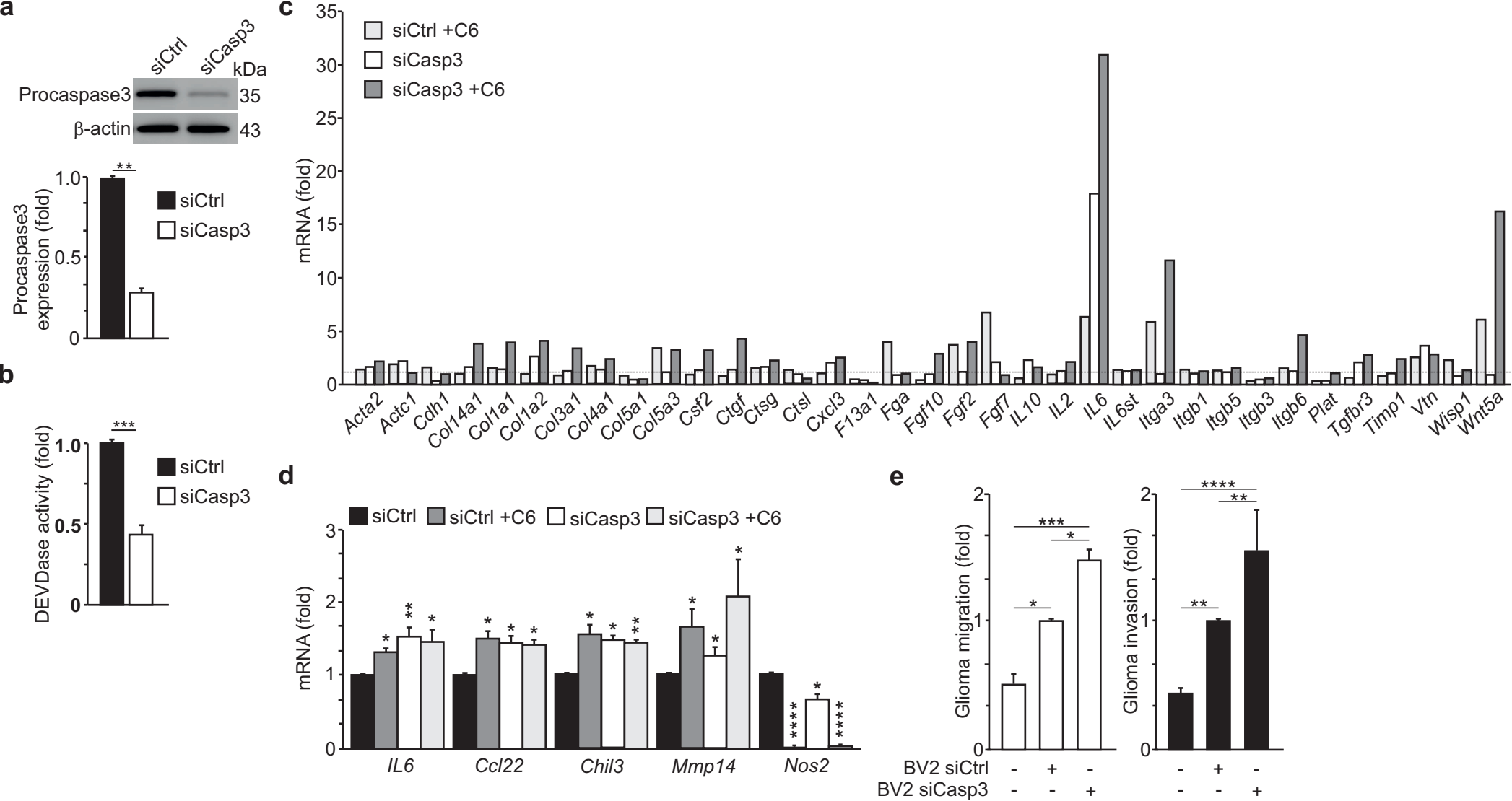
a
siCtrl
siCasp3
kDa
Procaspase3
35
β-actin
43
Procaspase3 expression (fold)
siCtrl
siCasp3
b
DEVDase activity (fold)
siCtrl
siCasp3
c
siCtrl +C6
siCasp3
siCasp3 +C6
mRNA (fold)
Acta2
Actc1
Cdh1
Col14a1
Col1a1
Col1a2
Col3a1
Col4a1
Col5a1
Col5a3
Csf2
Ctgf
Ctsg
Ctsl
Cxcl3
F13a1
Fga
Fgf10
Fgf2
Fgf7
IL10
IL2
IL6
IL6st
Itga3
Itgb1
Itgb5
Itgb3
Itgb6
Plat
Tgfbr3
Timp1
Vtn
Wisp1
Wnt5a
d
siCtrl
siCtrl +C6
siCasp3
siCasp3 +C6
mRNA (fold)
IL6
Ccl22
Chil3
Mmp14
Nos2
e
Glioma migration (fold)
Glioma invasion (fold)
BV2 siCtrl
BV2 siCasp3

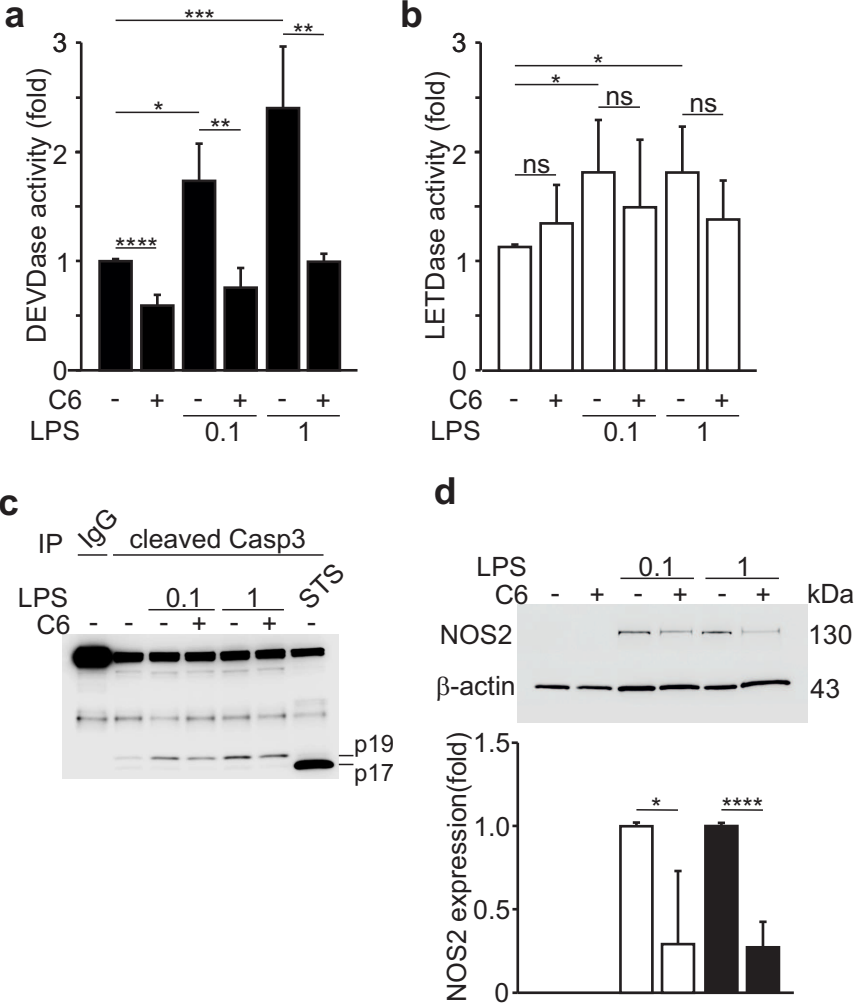
a
DEVDase activity (fold)
3
2
1
0
***
**
*
****
**
C6 - + - + - +
LPS 0.1 1
b
LETDase activity (fold)
3
2
1
0
*
*
ns
ns
ns
C6 - + - + - +
LPS 0.1 1
c
IP IgG cleaved Casp3
LPS 0.1 1 STS
C6 - - - + - + -
p19
p17
d
LPS 0.1 1
C6 - + - + - +
kDa
NOS2
130
β-actin
43
NOS2 expression(fold)
1.5
1.0
0.5
0
*
****

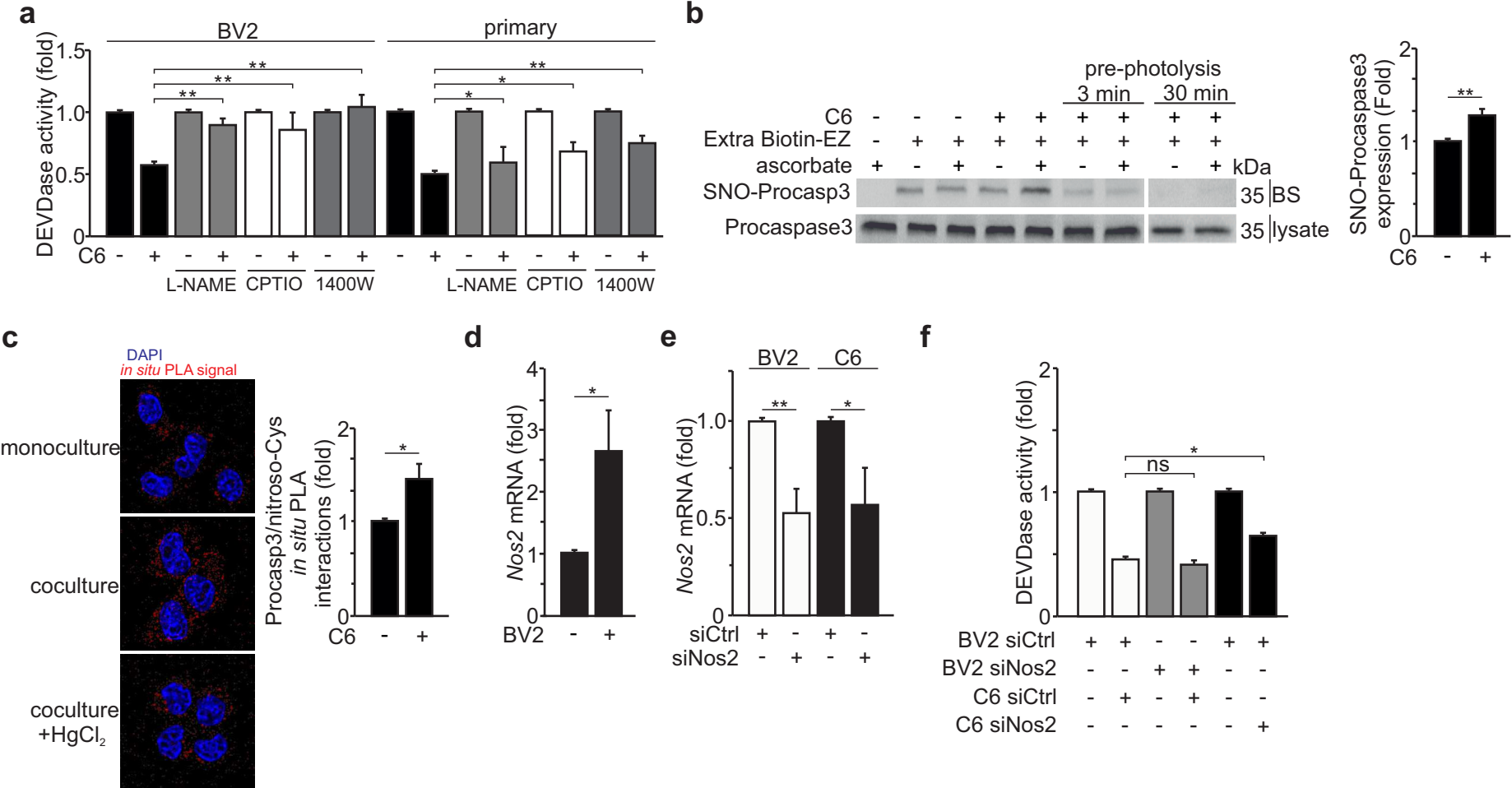
a
BV2
primary
DEVDase activity (fold)
1.5
1.0
0.5
0
**
**
**
*
*
**
C6 - + - + - + - + - + - + - + - +
L-NAME CPTIO 1400W
L-NAME CPTIO 1400W
b
pre-photolysis
3 min
30 min
C6 - - - + + + + + +
Extra Biotin-EZ - + + + + + + + +
ascorbate + - + - + - + - +
kDa
SNO-Procasp3
35 BS
Procaspase3
35 lysate
SNO-Procaspase3 expression (Fold)
2
1
0
**
C6 - +
c
DAPI
in situ PLA signal
monoculture
coculture
coculture +HgCl2
Procasp3/nitroso-Cys in situ PLA interactions (fold)
2
1
0
*
C6 - +
d
Nos2 mRNA (fold)
4
3
2
1
0
*
BV2 - +
e
BV2
C6
Nos2 mRNA (fold)
1.0
0.5
0
**
*
siCtrl + - + -
siNos2 - + - +
f
DEVDase activity (fold)
2
1
0
*
ns
BV2 siCtrl + + - - + +
BV2 siNos2 - - + + - -
C6 siCtrl - + - + - -
C6 siNos2 - - - - - +

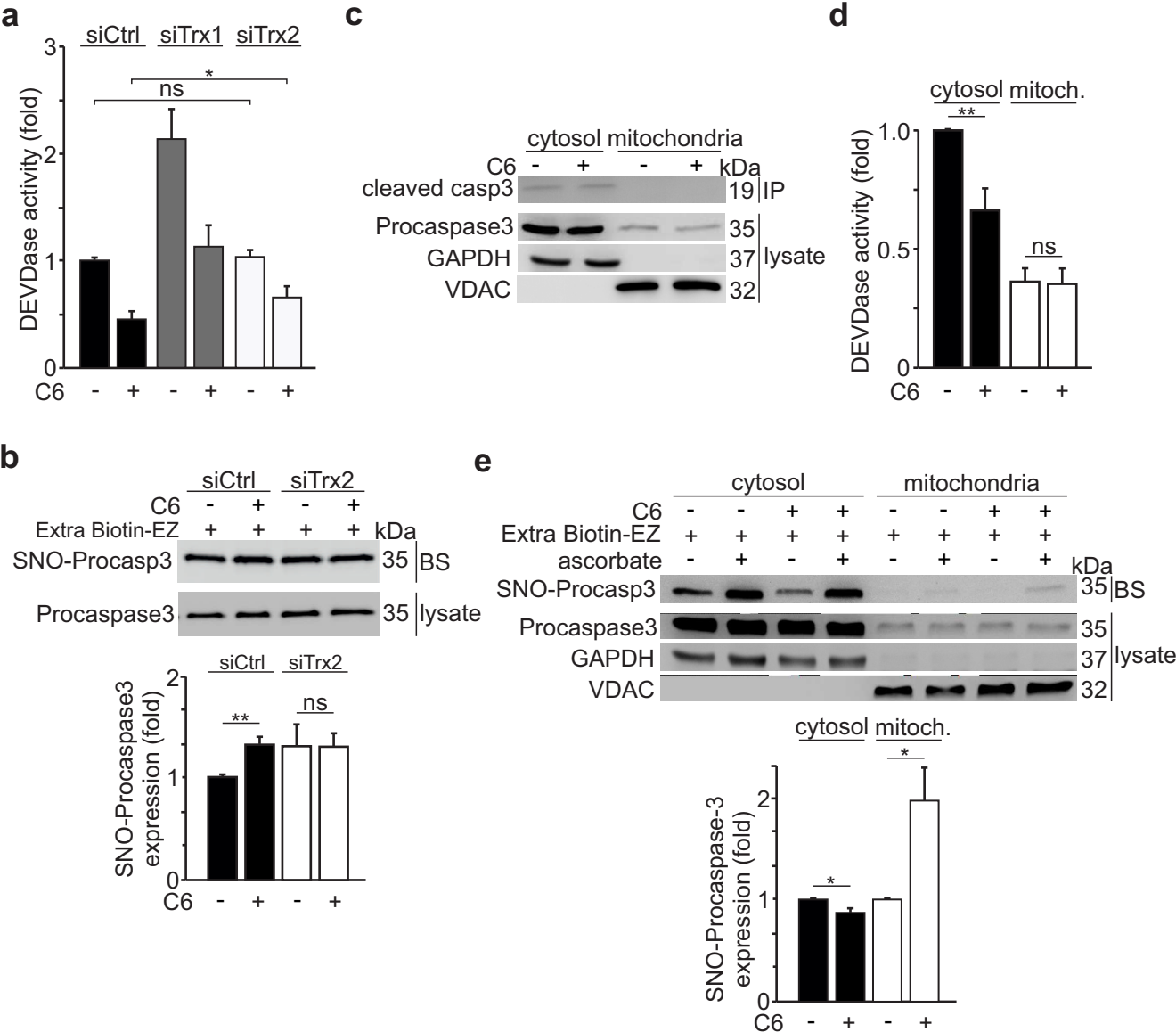
a
siCtrl
siTrx1
siTrx2
*
ns
DEVDase activity (fold)
3
2
1
0
C6 - + - + - +
c
cytosol
mitochondria
C6 - + - + kDa
cleaved casp3
19
IP
Procaspase3
35
GAPDH
37
lysate
VDAC
32
d
cytosol
mitoch.
**
ns
DEVDase activity (fold)
1.0
0.5
0
C6 - + - +
b
siCtrl
siTrx2
C6 - + - +
Extra Biotin-EZ + + + + kDa
SNO-Procasp3
35
BS
Procaspase3
35
lysate
siCtrl
siTrx2
**
ns
SNO-Procaspase3 expression (fold)
2
1
0
C6 - + - +
e
cytosol
mitochondria
C6 - - + + - - + +
Extra Biotin-EZ + + + + + + + +
ascorbate - + - + - + - +
kDa
SNO-Procasp3
35
BS
Procaspase3
35
GAPDH
37
lysate
VDAC
32
cytosol
mitoch.
*
*
SNO-Procaspase-3 expression (fold)
2
1
0
C6 - + - +

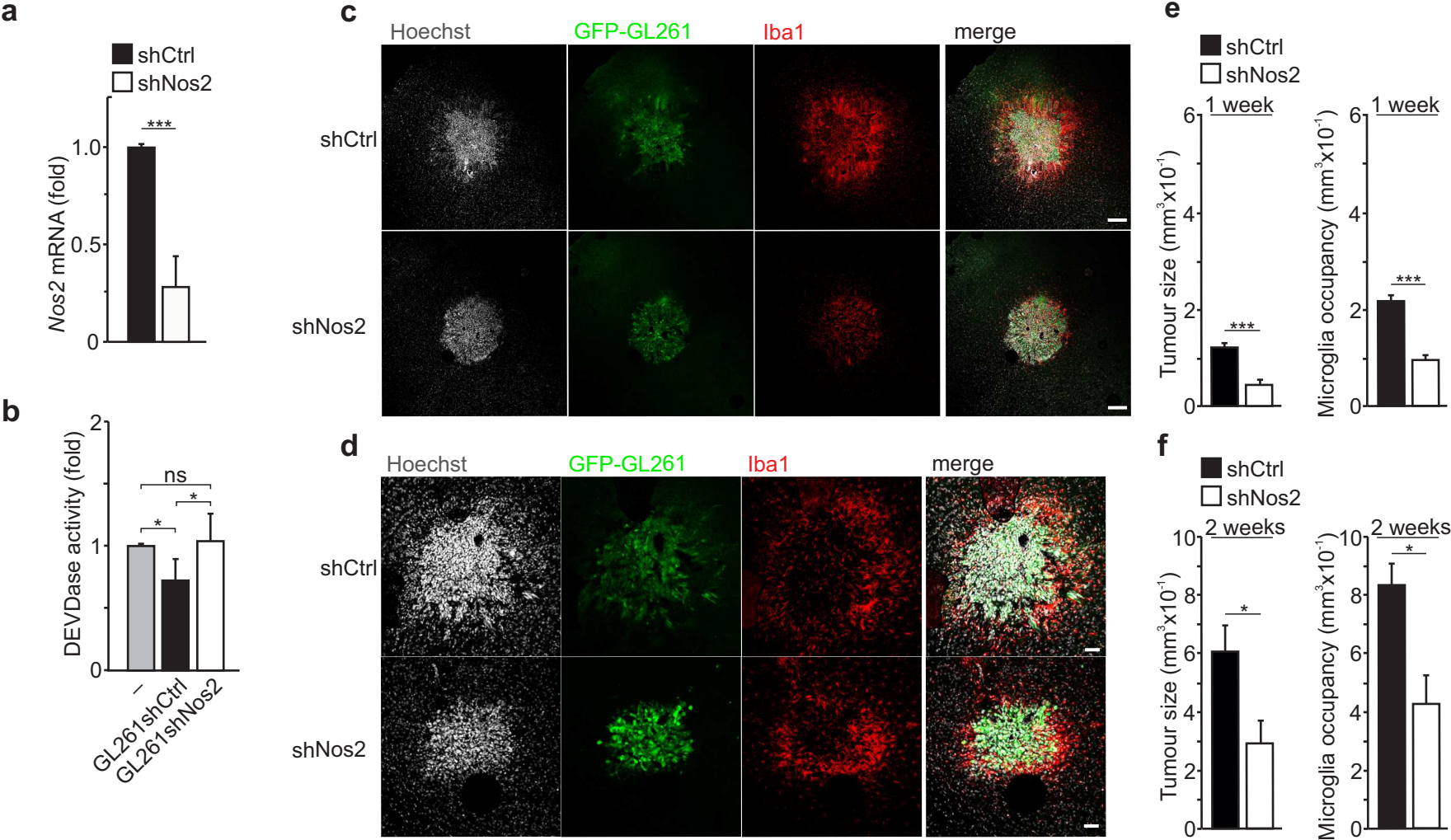
a
shCtrl
shNos2
***
Nos2 mRNA (fold)
1.0
0.5
0
b
DEVDase activity (fold)
2
1
0
ns
*
*
–
GL261shCtrl
GL261shNos2
c
Hoechst
GFP-GL261
Iba1
merge
shCtrl
shNos2
d
Hoechst
GFP-GL261
Iba1
merge
shCtrl
shNos2
e
shCtrl
shNos2
1 week
Tumour size (mm3x10-1)
6
4
2
0
***
1 week
Microglia occupancy (mm3x10-1)
6
4
2
0
***
f
shCtrl
shNos2
2 weeks
Tumour size (mm3x10-1)
10
8
6
4
2
0
*
2 weeks
Microglia occupancy (mm3x10-1)
10
8
6
4
2
0
*

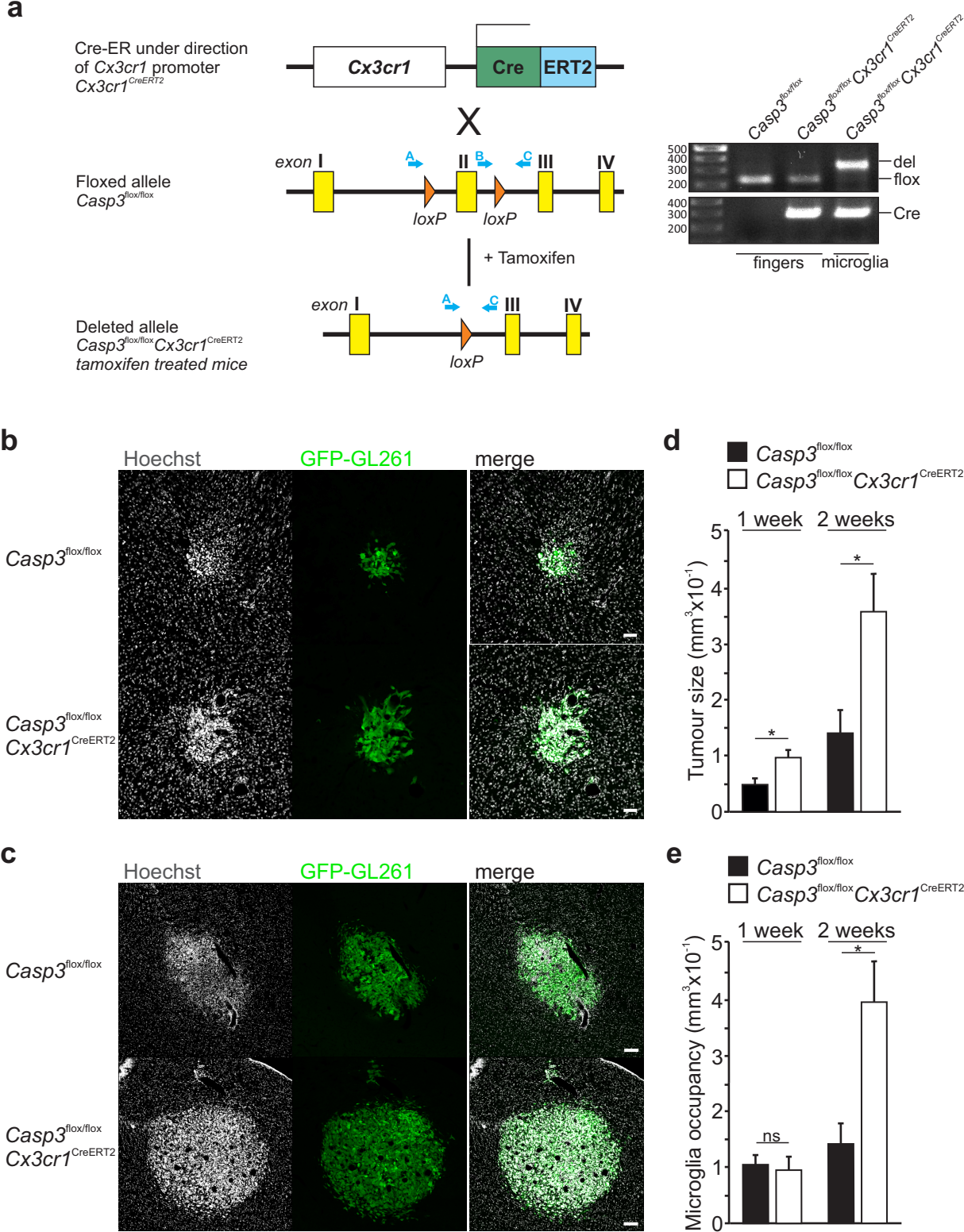
a
Cre-ER under direction of Cx3cr1 promoter
Cx3cr1CreERT2
Cx3cr1
Cre
ERT2
X
Floxed allele
Casp3flox/flox
exon I
II
III
IV
A
B
C
loxP
loxP
+ Tamoxifen
Deleted allele
Casp3flox/flox Cx3cr1CreERT2
tamoxifen treated mice
exon I
III
IV
loxP
Casp3flox/flox
Casp3flox/flox Cx3cr1CreERT2
Casp3flox/flox Cx3cr1CreERT2
500
400
300
200
del
flox
400
300
200
Cre
fingers
microglia
b
Hoechst
GFP-GL261
merge
Casp3flox/flox
Casp3flox/flox
Cx3cr1CreERT2
c
Hoechst
GFP-GL261
merge
Casp3flox/flox
Casp3flox/flox
Cx3cr1CreERT2
d
Casp3flox/flox
Casp3flox/flox Cx3cr1CreERT2
1 week
2 weeks
Tumour size (mm3x10-1)
5
4
3
2
1
0
*
*
e
Casp3flox/flox
Casp3flox/flox Cx3cr1CreERT2
1 week
2 weeks
Microglia occupancy (mm3x10-1)
5
4
3
2
1
0
ns
*